NEOPLASIA
www.neoplasia.com

Volume 18 Number 11 November 2016 pp. 699–710 699

# Upregulation of Glucose-Regulated Protein 78 in Metastatic Cancer Cells Is Necessary for Lung Metastasis Progression[1,2]

**Michael M. Lizardo*, James J. Morrow†,‡, Tyler E. Miller†,‡, Ellen S. Hong*, Ling Ren§, Arnulfo Mendoza*, Charles H. Halsey¶, Peter C. Scacheri†, Lee J. Helman* and Chand Khanna*,#**

*Pediatric Oncology Branch, Center for Cancer Research, National Cancer Institute, National Institutes of Health, Bethesda, MD, USA; †Department of Genetics and Genome Sciences, School of Medicine, Case Western Reserve University, Cleveland, OH, USA; ‡Department of Pathology, Case Western Reserve University, Cleveland, OH, USA; §Comparative Oncology Program, National Cancer Institute, National Institutes of Health, Bethesda, MD, USA; ¶Laboratory of Cancer Biology and Genetics, Center for Cancer Research, National Cancer Institute, National Institutes of Health, Bethesda, MD, USA; #Ethos Discovery in Washington DC and Ethos Veterinary Health, Wolburn MA, USA

## Abstract

Metastasis is the cause of more than 90% of all cancer deaths. Despite this fact, most anticancer therapeutics currently in clinical use have limited efficacy in treating established metastases. Here, we identify the endoplasmic reticulum chaperone protein, glucose-regulated protein 78 (GRP78), as a metastatic dependency in several highly metastatic cancer cell models. We find that GRP78 is consistently upregulated when highly metastatic cancer cells colonize the lung microenvironment and that mitigation of GRP78 upregulation via short hairpin RNA or treatment with the small molecule IT-139, which is currently under clinical investigation for the treatment of primary tumors, inhibits metastatic growth in the lung microenvironment. Inhibition of GRP78 upregulation and an associated reduction in metastatic potential have been shown in four highly metastatic cell line models: three human osteosarcomas and one murine mammary adenocarcinoma. Lastly, we show that downmodulation of GRP78 in highly metastatic cancer cells significantly increases median survival times in our *in vivo* animal model of experimental metastasis. Collectively, our data indicate that GRP78 is an attractive target for the development of antimetastatic therapies.

*Neoplasia (2016) 18, 699–710*

## Introduction

Significant strides have been made toward the improvement of overall survival in cancer patients with localized disease. Treatment of patients with metastatic disease, or at risk for metastatic progression, remains to be a challenge as metastases account for more than 90% of cancer-related deaths [1]. To develop effective antimetastatic therapeutics that address this unmet clinical need, further understanding of molecular drivers that allow a cancer cell to successfully complete all steps of the metastatic cascade is needed [2,3]. The lung is a common site of metastasis for many types of solid tumors including breast, prostate, melanoma, and pediatric osteosarcoma (OS). Pediatric OS is of particular interest because it is a solid tumor

Address all correspondence to Chand Khanna, Ethos Discovery, Washington DC and Ethos Veterinary Health, Woburn,MA.
E-mail: ckhanna@animalci.com

[1] Grant support: This research was supported (in part) by the Intramural Research Program of the National Institutes of Health, Center for Cancer Research, Pediatric Oncology Branch. M. M. L. was supported by National Institutes of Health Intramural Visiting Fellow Program (award 15335), J. J. M. and T. E. M. were funded by National Institutes of Health T32GM007250. J. J. M. and T. E. M. were also funded by National Institutes of Health/National Cancer Institute F30 CA186633 and CA183510, respectively. P. C. S. received grant support RO1CA160356.
[2] Disclosure of potential conflicts of interest: No potential conflicts of interest were disclosed by the authors of this study.
Received 16 May 2016; Revised 4 September 2016; Accepted 8 September 2016

1476-5586
http://dx.doi.org/10.1016/j.neo.2016.09.001

that overwhelmingly metastasizes to the lung [3] and, therefore, is a disease model that permits researchers to identify targets that influence lung metastatic progression [4]. Our laboratory has several OS models that have proved useful for gaining insight into some of the molecular pathways contributing to metastatic colonization of the lung by OS [4–6].

During the process of lung metastasis progression, the majority of tumor cells that disseminate to the lung fail to establish clinically detectable metastases [7]. Indeed, experimental data from our laboratory and other groups suggest that the majority of cancer cells that arrive in the lung microvasculature undergo apoptosis and that a common feature of highly metastatic cells is their unique ability to resist apoptosis in the lung [4,8]. In contrast, poorly metastatic cells show higher rates of apoptosis in this microenvironmental setting. These data suggest that metastatic cancer cells with a high metastatic potential are better adapted to meet the challenges of growing in the hostile microenvironment such as the lung. Indeed, such challenges may include 1) differences in oxygen tension, 2) reactive oxygen and nitrogen species, and 3) differences in nutritional sources [4,9]. To successfully establish overt metastasic tumors in the lung, metastatic cancer cells must quickly adapt to fluctuations in microenvironment and maintain cellular homeostasis as they arrive and grow within this hostile microenvironment [10,11]. To understand how metastatic cancer cells adapt to the lung microenvironment, we turn our attention to the endoplasmic reticulum (ER) because it is known to be a central organelle in both sensing a variety of cellular stresses and initiating homeostatic responses that attempt to ameliorate the stress or commit the cell to apoptosis [12].

The ER is an extensive tubular network that extends throughout the cell and is the site where one third of all cellular proteins are produced and processed [12]. Protein folding and chaperone activity within the ER are dependent on multiple factors including 1) ATP supply, 2) redox state, 3) $Ca^{2+}$ levels, and 4) nutrients supply, all of which make ER function exquisitely sensitive to external environmental conditions [13,14]. When adverse environmental conditions interfere with ER function, misfolded/unfolded proteins accumulate (a condition known as ER stress). ER membrane "stress sensors" (IRE1, PERK, and ATF6) detect ER stress and initiate a transcriptional program that increases ER function by upregulating foldases, chaperones, and co-chaperones. Glucose-regulated protein 78 (GRP78) is a major ER molecular chaperone that is upregulated during this adaptive response, and participates in protein folding and prevents protein aggregation [15]. GRP78 is found to be upregulated in many types of cancers [16]. GRP78 upregulation has been associated with chemoresistance [17,18], and interestingly, the protein itself has been found to have antiapoptotic activity in breast cancer cells [19]. Considering the microenvironmental stresses metastatic cancer cell encounters in the lung and how the ER plays a major role in the induction of cellular adaption to such stresses, it is reasonable to hypothesize that the adaptive ER-stress response, particularly the upregulation of GRP78, is required for an aggressive highly metastatic phenotype.

The following report provides the first functional link between the induction of an adaptive ER-stress response (GRP78 upregulation) and an aggressive metastatic phenotype. More specifically, highly metastatic cancer cells differentially upregulate GRP78 compared with poorly metastatic cancer cell when growing in the lung or when challenged with pharmacological drugs that induce ER stress *in vitro*. Moreover, GRP78 upregulation is linked to metastatic aggressiveness because inhibition of GRP78 results in lower lung tumor burden and higher median survival times in our animal models. Collectively, these data suggest that GRP78 upregulation in metastatic cancer cells is a critical driver of their metastatic success and that the capacity of metastatic cancer cells to elicit this response directly correlates with metastatic potential. Our observations add an important translational rationale to the clinical development of therapeutic agents (i.e., IT-139) that target these ER-stress adaptation pathways. These data and treatment rationale are well aligned with the recent recognition of the importance for drug development approaches that target metastatic progression in cancer patients.

## Materials and Methods

### *Cell Culture and Materials*

Human OS cell lines MG63, MNNG, HOS, and 143B and the murine mammary carcinoma cell lines 4T1 and 67NR were all obtained from ATCC. MNNG, 143B, and 4T1 cells are characterized to have a highly metastatic phenotype *in vivo* [20,21]. The MG63.3 cell line is a highly metastatic clonal variant of the human OS cell line established from MG63.2 cells, which were in turn established from the MG63 cell line [21]. The MG63, HOS, and 67NR cell lines were previously characterized to have a poorly metastatic phenotype *in vivo* [20]. To visualize cells by fluorescence microscopy, all cells were transduced with enhanced green fluorescent protein (eGFP) where the cytomegalovirus promoter (for human cells) or *pol II* promoter (for murine cells) was used to drive eGFP expression. The MG63, MG63.3, HOS, MNNG, and 143B cell lines were authenticated by short tandem repeat DNA profiling at the University of Colorado DNA Sequencing and Analysis Core in September 2014. 4T1 and 67NR cells that were originally obtained from ATCC have not been authenticated further. All cell lines are routinely tested for mycoplasma contamination using the Lonza MycoAlert Plus. The small molecule inhibitor of GRP78 expression IT-139 was kindly provided by Intezyne. All cell lines were maintained in Dulbecco's modified essential medium (Invitrogen) containing 10% fetal bovine serum, 5% penicillin/streptomycin (100 U/ml) at 37°C, and 5% $CO_2$.

### *Transcriptome Profiling of Highly Metastatic Cells and Poorly Metastatic Cells Grown in 2D Cell Culture and in the Lung*

To survey and compare the expression of ER-stress responsive genes in highly metastatic cells and poorly metastatic tumor cells growing in 2D cell culture conditions or in the lung, tumor cell RNA was isolated from cells growing in cell culture plates, as well as from early and later stages of metastasis in the pulmonary metastasis assay (PuMA) model (1 day and 14 days postinjection), as described by Morrow and colleagues [22]. Briefly, RNA was isolated from MG63.3 and MG63 cells growing in cell culture plates by the standard TRIzol method. Because the contrasting growth kinetics of the MG63.3/MG63 pair were previously well characterized in the PuMA model, we decided to obtain RNA material from MG63.3 or MG63 growing in the lung at early and late time points in the progression of metastatic growth. PuMA lung sections containing eGFP-expressing tumor cells were physically minced with fine scissors and digested with 1 mg/ml of collagenase (Roche) in Hank's balanced salt solution at 37°C for 30 minutes. The digestion was stopped by adding 10 mM EDTA. The lung digest was homogenized by passing through an 18G needle attached to a 10-ml syringe and passed

through a 70-μm cell strainer. The homogenate was centrifuged at 500 ×*g* for 5 minutes at 4°C. The supernatant was aspirated, and cell pellet was resuspended in 5 ml of ammonium-chloride-potassium lysing buffer for 3 minutes at room temperature to lyse red blood cells. Red blood cell lysis was stopped by adding 10 ml of Hank's balanced salt solution, and cells were centrifuged for 5 minutes at 4°C. The supernatant was discarded, and cells were resuspended in 3 ml of PBS with 0.5 mM EDTA and placed on ice. eGFP-positive MG63.3 and MG63 cells were isolated by fluorescent activated cell sorting. Sorted eGFP human OS cells were centrifuged, the cell pellet was lysed in 1 ml of TRIzol reagent (Life Technologies), and RNA was isolated using standard procedures using chloroform. RNA samples were further processed using the RNAeasy Micro Kit (Qiagen). RNA quality was assessed using a 2200 Tapestation Instrument (Agilent). PolyA+ RNA was prepared by using the Illumina Truseq RNA Sample Preparation kit as per manufacturer's instructions. Samples were sequenced using the Illumina HiSeq 2500 platform.

To find ER-stress responsive genes that were preferentially upregulated only in highly metastatic versus poorly metastatic cancer cells in the lung, RNA sequencing data were parsed using a list of genes known to have ER-stress elements in their promoter regions [23]. This approach was used to identify specific parts of ER-stress signaling pathway that may be mechanistically linked to a role for ER stress response in metastasis. From this initial data set, the expression profiles of a smaller subset of genes were chosen based on their differential upregulation in highly metastatic cells versus poorly metastatic cells in the lung microenvironment. The expression profiles of these differentially upregulated genes were represented in a smaller heat map.

### *Fluorescence Immunostaining and Confocal Imaging*

For paraffin tissue sections, sections were dewaxed with xylene and rehydrated with an alcohol series. Antigen retrieval was performed by heating the slides at 95°C for 25 minutes in a working solution of Target Retrieval Solution (DAKO). The slides were permeabilized with phosphate-buffered saline with 0.01% Triton for 10 minutes. Slides were blocked with 4% bovine serum albumen in phosphate-buffered saline with 0.01% Triton for 10 minutes. To detect eGFP-expressing human tumor cells in tissue sections, primary goat antibodies (against eGFP) directly conjugated to fluorescein isothiocyanate (Abcam) were used. To detect GRP78, polyclonal rabbit anti-GRP78 antibodies (1:100, Abcam) were used. Goat anti-rabbit secondary antibodies conjugated to Alexa 594 were used to localize rabbit anti-GRP78 in tissue sections. Nuclei were counterstained blue with 4′,6-diamidino-2-phenylindole (DAPI, 1 mg/ml; Sigma) for 5 minutes. Tissue sections stained only with secondary antibodies served as omission controls to assess the level of background fluorescence. Tissue sections were imaged using a Zeiss 710 laser scanning confocal microscope equipped with argon, DPSS 561, and Diode 405 lasers, where images were acquired using either a low-power (20×) objective lens or 63× oil immersion objective lens.

### *Stereological Analysis of GRP78 Expression in Metastatic OS Cells in Culture and in the Lung In Situ*

GRP78 expression in metastatic cancer cells both in 2D cell culture and in lung tissue sections was quantified using a dimensionless stereological parameter called area fraction ($A_A$). Described by Underwood [24], $A_A$ is assessed on a per-cell basis and is calculated by assessing the GRP78 (Alexa 594 red fluorescence) staining area divided by the area of the cell (fluorescein isothiocyanate, green fluorescence). The average area fraction of GRP78 per cell was calculated and compared between highly metastatic cells and poorly metastatic tumor cells growing in 2D culture *in vitro* and in paraffin tissue sections of PuMA lung slices taken at 0 and 14 days postinjection; 20 to 80 tumor cells were counted per condition.

### *Western Blotting*

The protein concentration for cell lysates were determined by the bicinchoninic assay (ThermoFisher), as per manufacturer's instructions. Fifteen or twenty micrograms of protein was loaded in 4% to 20% mini-gel (Invitrogen) and electrophoresed for 150 minutes at 120 V and 40 mA. After electrophoresis, gels were placed in iBlot Gel Transfer Device (Invitrogen), and proteins were transferred to a nitrocellulose membrane. Prior to the addition of primary antibodies, membranes were blocked in TRIS-buffered saline with 0.1% Tween-20 and 5% milk powder for 1 hour. Antibodies against rabbit anti-GRP78 (1:1000, Abcam) and mouse anti-β-actin (Sigma-Aldrich) were incubated overnight at 4°C. Membranes were washed with TRIS-buffered saline with 0.1% Tween-20 and incubated with either goat anti-rabbit or goat-anti-mouse IgG conjugated to horseradish peroxidase (Sigma-Aldrich). Protein bands were visualized on film using the Supersignal West Pico Chemiluminescent Substrate Kit (ThermoFisher) per manufacturer's instructions.

### *Image Cytometry of GRP78 Expression between Highly Metastatic Cells and Poorly Metastatic Tumor Cells under ER Stress Conditions In Vitro*

For a high-throughput quantitative analysis of how populations of highly metastatic cells and poorly metastatic tumor cells modulate GRP78 expression in response to ER stress, immunofluorescence staining and single-cell image cytometry were used to quantify GRP78 expression in highly metastatic cells and poorly metastatic cells following exposure to tunicamycin. Briefly, $4 \times 10^5$ highly metastatic cells and poorly metastatic cells were treated with vehicle, 50 nM tunicamycin, or 100 nM tunicamycin for 24 hours. The next day, vehicle- and tunicamycin-treated cells were trypsinized, washed with PBS, and fixed in cell suspension with 4% paraformaldehyde in PBS for 12 minutes. Fixed cells were then suspended in solution of polyclonal rabbit anti-GRP78 antibodies (1:100) in blocking buffer and incubated overnight at 4°C. For secondary detection, goat anti-rabbit secondary antibodies conjugated to phycoerythrin were used. Stained cells were analyzed using a Cellometer Vision CBA Image Cytometry System equipped with fluorescence. Image analysis of micrographs of fluorescent stained cells was automated by using FCS 4 Express Flow Plus Image software (DeNOVO). The number of cells counted typically ranged from 800 to 2000 for each condition, and the experiment was repeated twice.

### *GRP78 Knockdown with Lentiviral TET-ON Inducible Short Hairpin RNA (shRNA) or IT-139 Treatment*

The TET-ON (doxycycline) inducible vector used in this study is based on the previously published shRNAmir, "miR-E," pRRL backbone [25]. The lentiviral version of the vector, LT3REVIR (a kind gift from Dr. Zuber), which couples the induction of shRNA with the expression of red fluorescent protein (dsRED), was modified by replacing the constitutively active fluorescent reporter *venus* gene with a *pac* (puromycin resistance) gene which enables eukaryotic selection. Two different shRNAs against GRP78 were selected from the transOMIC technologies shERWOOD-UltramiR shRNA

library. Cloning of shRNA into backbone construct was performed on contract by transOMIC Technologies. The following two shRNA antisense sequences, which target the coding region of GRP78 mRNA, were evaluated: shGRP78_1 (TATATCAACTTGAATG TATGGT) and shGRP78_2 (TTAGCTTTGAAGTCTT CAATGT). Ready-made lentiviral particles containing the modified lentiviral expression vector were prepared by standard methods using HEK cells and packaging plasmids (transOMIC Technologies). For transduction, MG63.3 or MNNG ($2 \times 10^5$ cells/well) cells were seeded in a 6-well plate 1 day before transfection. The cells were transfected with lentiviral particles with a multiplicity of infection = 5. A nontargeting shRNA was used for the control. Transduced cells were placed under selection with 2 μg/ml of puromycin for 3 days, at which time untransduced cells were no longer surviving. After a week of selection, over a hundred colonies of puromycin-resistant cells formed which were subsequently pooled into one population. GRP78 protein expression in MG63.3 cells and MNNG cells is low at baseline but is upregulated when cells are exposed to a pharmacological ER stressor (i.e., tunicamycin). Therefore, we assessed the efficiency of knockdown in MG63.3 and MNNG cells that were treated with tunicamycin (50 nM) for 24 hours in the presence (doxycycline, 5-μg/ml treatment for 96 hours) or absence of doxycycline. For subsequent tail-vein injection experiments that assessed the metastatic potential of MG63.3 cells and MNNG cells (where shRNA and dsRED were induced by doxycycline treatment), cell populations were enriched for cells double-positive for eGRP and dsRED by using a fluorescence-activated cell sorting machine, MoFlo Astrios (Beckman Coulter), equipped with 488-nm and 561-nm lasers to sort GFP and RFP cells, respectively.

To pharmacologically downmodulate GRP78, cancer cells were treated with the small molecule drug IT-139 (formally NKP-1339, kindly provided by Intezyne) which has been characterized to inhibit GRP78 expression [26]. Inhibition of GRP78 induction (via 50-nM tunicamycin treatment) was tested at 10, 50, 100, and 200 μM IT-139 for 24 hours. These conditions were previously found to have little effect on cell proliferation. Cell lysates were collected (as previously described), and knockdown of GRP78 levels was assessed by Western immunoblotting.

### *Pulmonary Metastasis Assay*

To directly visualize metastatic cancer cell growth in the lung and to assess the effects of GRP78 downmodulation on metastatic growth over time, we used an *ex vivo* lung explant model called the PuMA as described by Mendoza and colleagues [27]. Briefly, eGFP-expressing cancer cells ($3 \times 10^5$ cells for MG63.3, $2.5 \times 10^5$ cells for MNNG, $3 \times 10^5$ cells for 4T1 cells) were seeded in the lung of severe immune compromised mice (SCID, Charles River) *via* tail vein injection. The mouse was euthanized, and the lung was insufflated with 37°C 50:50 liquid mixture of media and 1.2% low-melting point agarose (Lonza) by gravity perfusion. The agarose-filled lungs were allowed to solidify in ice-cold PBS for 20 minutes. After the lungs solidified, fine scissors and forceps were used to cut small lung slices (2 mm × 4 mm) which were used for longitudinal imaging using a lower-power objective (50× magnification) microscope. Metastatic growth for each cell line/condition was longitudinally monitored over 14 days. For doxycycline treatment or IT-139 treatment for 14 days, media and drug were replenished every second day. For each lung slice, the stereological parameter area fraction ($A_A$) was calculated (see *Stereological Analysis of GRP78 Expression in Metastatic OS cells in Culture and in the Lung In Situ* section for details). For drug studies and genetic knockdown studies, 4 to 10 lung slices from 1 mouse were used per condition. PuMA experiments were repeated three times. When lung slices were to be imaged, lung slices were placed in a small culture dish with a glass coverslip bottom using aseptic technique and then imaged on a Leica DM IRB Widefield Fluorescence Microscope equipped with a filter set appropriate for imaging eGFP.

### *In Vivo Experimental Metastasis Studies*

All *in vivo* animal studies using SCID mice were performed with the approval of the Animal Care and Use Committee of the National Cancer Institute. For experimental metastasis survival studies, 5 groups of mice ($n = 10$) were studied: group 1 consisted of mice injected with $3 \times 10^5$ human MG63.3 shGRP78_1 cells without pretreatment of doxycycline, and mice were kept on a normal diet; group 2 consisted of mice injected with $3 \times 10^5$ human MG63.3 shGRP78_1 cells with pretreatment of doxycycline (for 5 days), and mice were kept on a chow with doxycycline (2 g/kg); group 3 consisted of mice injected with $3 \times 10^5$ human MG63.3 cells shGRP78_2 cells without pretreatment of doxycycline, and mice were kept on a normal diet; group 4 consisted of mice injected with $3 \times 10^5$ human MG63.3 shGRP78_2 cells with pretreatment of doxycycline, and mice were kept on a doxycycline-chow diet; group 5 consisted of mice injected with $3 \times 10^5$ human MG63.3 cells with a nontargeting control shRNA with pretreatment of doxycycline (for 5 days), and mice were kept on a doxycycline-chow diet. End point for individual mice was reached when mice showed signs of labored breathing from lung metastases or if there was no metastasis-related death at 60 days. Necropsy at end point allowed the identification and validation of pulmonary metastases in all mice. Whole lungs with the metastases were imaged under fluorescence using a Leica MZ FLIII Stereo-Fluorescence Dissecting Microscope equipped with a fluorescence light source.

### *Assessment of GRP78 Expression in Human OS*

Immunohistochemical staining for GRP78 (Abcam) was performed on a patient-derived tissue microarray (TMA) described by Osborne and colleagues [28]. Paraffin TMA slides were processed as previously described (see *Fluorescence Immunostaining and Confocal Imaging* section). TMA slides were stained with primary antibodies against GRP78 (Abcam) and the EnVision + System Kit (Dako) as per manufacturer's instructions. A TMA slide stained without primary anti-GRP78 antibodies served as an omission control to assess the level of background staining. TMA slides were digitally scanned with a digital whole-slide scanner (Aperio ScanScope XT; Aperio Technologies) using a 20× objective and annotated and reviewed in Aperio ImageScope. Quantification of GRP78 labeling was conducted on each tissue core using the CytoNuclear Tool (Indica Laboratories) computer image analysis algorithm. Custom settings for the CytoNuclear Tool algorithm were determined by a pathologist prior to analysis. GRP78 expression was recorded as both a percentage of positively labeled cells per core and the percentage of cores expressing GRP78.

### *Statistical Analysis*

Statistical analysis data were performed using Graph Prism Statistical Software P. For data with a normal distribution, the means were analyzed by either unpaired *t* test or one-way analysis of variance to compare multiple groups. For *post hoc* analysis, Tukey's multiple comparisons test was used to assess which means were significantly

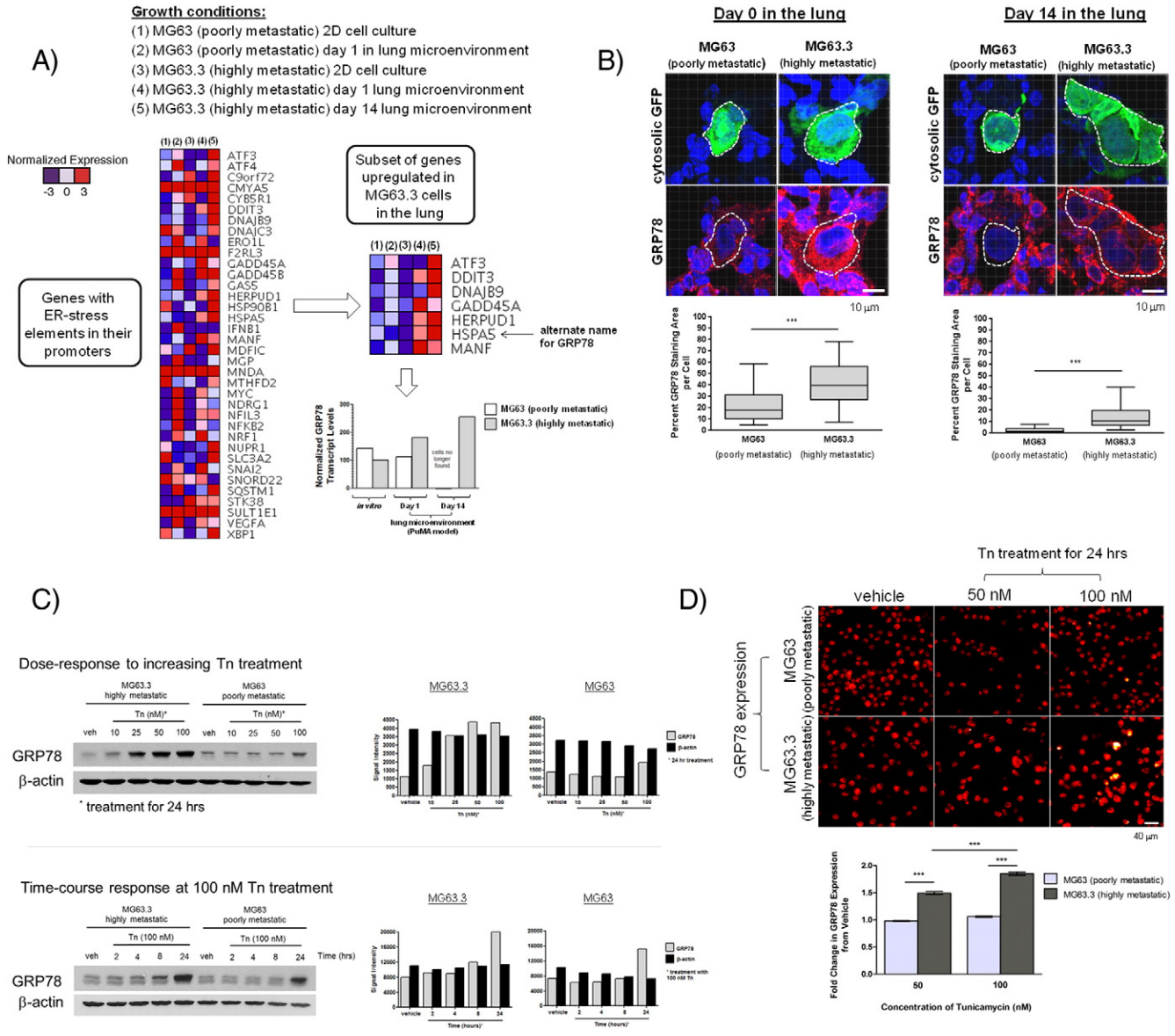


**Figure 1.** Differential upregulation of the ER chaperone protein GRP78 in highly metastatic MG63.3 cells versus poorly metastatic MG63 cells in the lung microenvironment. (A) Relative transcript levels of genes with ER-stress elements in their promoters in MG63.3 and MG63 cells isolated from 2D *in vitro* cell culture conditions or from growing in the PuMA model at days 1 and 14 (larger heat map). A smaller subset of genes (one of which is *GRP78*) was differentially upregulated in MG63.3 versus MG63 only in the lung. Normalized GRP78 transcript levels are represented in the bar graph. (B) Representative confocal images of GRP78 immunofluorescence staining within OS cells in lung tissue sections (PuMA model) at days 0 and 14 are shown. Triple-color immunofluorescence staining was used to show the location of OS cells (green) and GRP78 (red); nuclei were counterstained with DAPI (blue). Dashed white lines delineate where GFP-expressing OS cells are located, and the corresponding GRP78 expression in these OS cells is shown below. Scale bar = 10 $\mu$m. GRP78 staining in MG63.3 and MG63 cells was quantified and compared for days 0 and 14, as shown in the box and whisker plot (5%-95% percentile). Mann-Whitney *U* test, $P < .001$. (C) Western blot showing *in vitro* differential upregulation of GRP78 in MG63.3 versus MG63 cells upon 24-hour treatment with tunicamycin (Tn). Densitometry measurements of the Western blots for MG63.3 and MG63 cells are also shown: gray bars denote GRP78 levels; black bars show β-actin as a loading control. A time-course Western blot experiment showing increasing exposure times of tunicamycin at 100 nM from 0 to 24 hours is shown. Densitometry measurements of the time-course Western blots for MG63.3 and MG63 cells are also shown: gray bars denote GRP78 levels; black bars show β-actin as a loading control (D) Image cytometry-based immunofluorescence quantification of GRP78 expression in MG63.3 and MG63 cells treated with tunicamycin for 24 hours. Representative micrographs are shown. Scale bar = 40 $\mu$m. Quantification of the fold-change in the fluorescence (normalized to vehicle) is shown in the bar graph. Mean and standard error of the mean are shown. The number of cells analyzed per group ranged from 1791 to 4090 cells. Kruskal-Wallis test, $P < .0001$; Dunn's multiple comparisons test, $P < .05$.

different. For data with nonnormal distribution, medians were compared by either Mann-Whitney *U* test or Kruskal-Wallis one-way analysis of variance. For *post hoc* analysis of medians, Dunn's multiple comparisons test was used. For experimental metastasis survival studies, data were analyzed using log-rank test. *P* values less than .05 were regarded as statistically significant. Mice that did not have any tumor burden in the lung at the defined end point of 60 days were censored from the survival data analysis.

## Results

### *Subset of ER-Stress Responsive Genes Is Upregulated in Highly Metastatic Cancer Cells in Lung*

To ascertain whether the ER-stress adaptive response is induced in metastatic cancer cells when growing in lung tissue of our PuMA (see *Materials and Methods*), eGFP-expressing metastatic cancer cells were isolated from homogenized lung tissue by FACS, and RNA was extracted for RNA sequencing. We examined changes in expression of genes with ER-stress response elements in their promoter region [23] (larger heat map, Figure 1*A*). We further identified a smaller subset of ER-stress responsive genes that were upregulated in highly metastatic cancer cells versus poorly metastatic cancer cells when in the lung microenvironment (smaller heat map, Figure 1*A*). Of these upregulated genes, GRP78 (also known as heat shock protein A5) was observed to be consistently upregulated in three highly metastatic OS cell lines when growing in the lung microenvironment: MG63.3 cells (smaller heat map, Figure 1*A*), MNNG cells (smaller heat map, Supplementary Figure 2*A*), and 143B cells (smaller heat map, Supplementary Figure 3*A*). Normalized GRP78 transcript levels between MG63.3 and MG63 *in vitro* and when growing in the lung microenvironment at days 1 and 14 in the PuMA model are shown in the bar graph in Figure 1*A*. These data show that the upregulation of a subset of ER-stress associated genes (especially *GRP78*) is a common feature of highly metastatic cancer cells.

### *Confocal Imaging and Validation of GRP78 Upregulation in Highly Metastatic Cells Growing in the Lung*

To validate the GRP78 transcript data at the protein level, *in situ* GRP78 expression in metastatic cancer cells was assessed *via* immunofluorescence staining and confocal microscopy (Figure 1*B*). Image analysis reveals that highly metastatic MG63.3 cells have a significantly larger area of GRP78 staining per cell (~42%) compared with poorly metastatic MG63 cells (~22%) during the initial stages of colonization in the PuMA model (day 0). Elevated levels of GRP78 in MG63.3 cells versus MG63 cells persist to day 14 in the PuMA model (Figure 1*B*). In contrast, when MG63.3 cells and MG63 cells are grown in 2D, *in vitro* cell culture conditions, the average percent staining area of GRP78 per cell is similar between the two cell lines (Supplementary Figure 1, *A* and *B*). The specificity of GRP78 fluorescent staining was validated by showing spatial overlap with calnexin, another marker of the ER [29]. GRP78 staining was shown to overlap with calnexin in cells grown *in vitro* (Supplementary Figure 2*A*) and *in situ* PuMA lung sections (Supplementary Figure 2*B*). Collectively, these results show that GRP78 staining area per tumor cell is greater in highly metastatic cells compared with poorly metastatic cancer cells only when growing in the lung microenvironment.

### *Highly Metastatic Cancer Cells Have A Higher Fold-Change of GRP78 Compared with Poorly Metastatic Cancer Cells under ER Stress Conditions In Vitro*

When treated with increasing concentrations of tunicamycin for 24 hours, highly metastatic cells showed elevated GRP78 expression relative to poorly metastatic cells (dose-response upper blots in Figure 1*C*). A time-course study looking at GRP78 expression at increasing exposure times in response to 100-nM tunicamycin treatment also shows a higher accumulation of GRP78 in MG63.3 cells versus MG63 cells (time-course lower blots in Figure 1*C*). The differential expression of GRP78 in response to increasing concentrations of tunicamycin was also observed by Western blotting in two other human, highly metastatic OS cell lines: MNNG cells (Supplementary Figure 3*B*) and 143B cells (Supplementary Figure 4*B*). High-throughput immunofluorescence-based quantification of GRP78 expression at the single cell level (Figure 1*D*) demonstrates that highly metastatic MG63.3, when normalized to vehicle treatment, exhibited a significantly higher fold change in GRP78 expression compared with poorly metastatic MG63 cells. These data show that highly metastatic cancer cells have a greater capacity to respond to ER stress compared with poorly metastatic cancer cells.

### *Downmodulation of GRP78 in Highly Metastatic Cancer Cells Inhibits Their Ability to Colonize Lung Tissue*

A schematic of the doxycycline-inducible shRNA lentiviral vector used to downmodulate GRP78 is shown in Figure 2*A*. Two different shRNAs predicted to inhibit GRP78 expression, and a non-targeting control, were used to address the concern of off-target effects. The GRP78 levels following shRNA knockdown is shown by Western blotting and densitometry (Figure 2, *B* and *C*). At baseline, GRP78 expression is low in untreated and doxycycline-treated MG63.3 cells. Only when GRP78 upregulation was induced by tunicamycin treatment did we see a reduction in GRP78 protein levels in doxycycline-treated MG63.3 cells. Because GRP78 is posttranslationally modified by phosphorylation and ADP-ribosylation, Western bands can be seen as doublets or triplets [30]. Downmodulation of GRP78 showed nominal effects on cell proliferation with shGRP78_2 and the nontargeting control shRNA having a modest effect on cell growth (Figure 2*C*), indicating that elevated expression of GRP78 is not necessary for cell survival in the absence of stress. In the context of lung microenvironment of the PuMA model, however, both shGRP78_1 and shGRP78_2 (when induced with doxycycline) significantly inhibited the ability of MG63.3 cells to colonize lung tissue (Figure 2, *B* and *C*). In contrast, the nontargeting shRNA controls (Figure 2*D*) did not inhibit the upregulation of GRP78 after tunicamycin treatment and did not prevent outgrowth of metastatic cancer cells in the lung. Downmodulation of GRP78 protein levels inhibiting metastatic outgrowth in the PuMA model was recapitulated using the small molecule drug IT-139 (Figure 2*E*). Treatment of MG63.3 cells with increasing concentrations of IT-139 showed a corresponding decrease in GRP78 protein levels. Treatment of MG63.3 cells growing in lung tissue in the PuMA model inhibited their outgrowth. We confirmed that inhibition of GRP78 expression by shRNA or IT-139 treatment significantly inhibited metastatic outgrowth in two other highly metastatic human OS cell line models: MNNG, which was derived separately from the HOS cell line (Supplementary Figure 3, *C*–*E*), and the highly metastatic 143B cells that were also derived from HOS cells (Supplementary Figure 4*C*). Collectively, the results indicate that GRP78 upregulation is required for successful colonization of the lung by highly metastatic human OS cells.

### *Downmodulation of GRP78 via shRNA Knockdown in Highly Metastatic OS Cells Extends Median Survival Times In Vivo*

A schematic of the *in vivo* experimental metastasis survival study where we ascertained the effects of GRP78 knockdown using two different shRNAs against GRP78 and a nontargeting scramble control RNA on median animal survival is outlined in Figure 3*A*. We found that mice that harbored tumors containing doxycycline-induced shGRP78_1 or shGRP78_2 had a longer

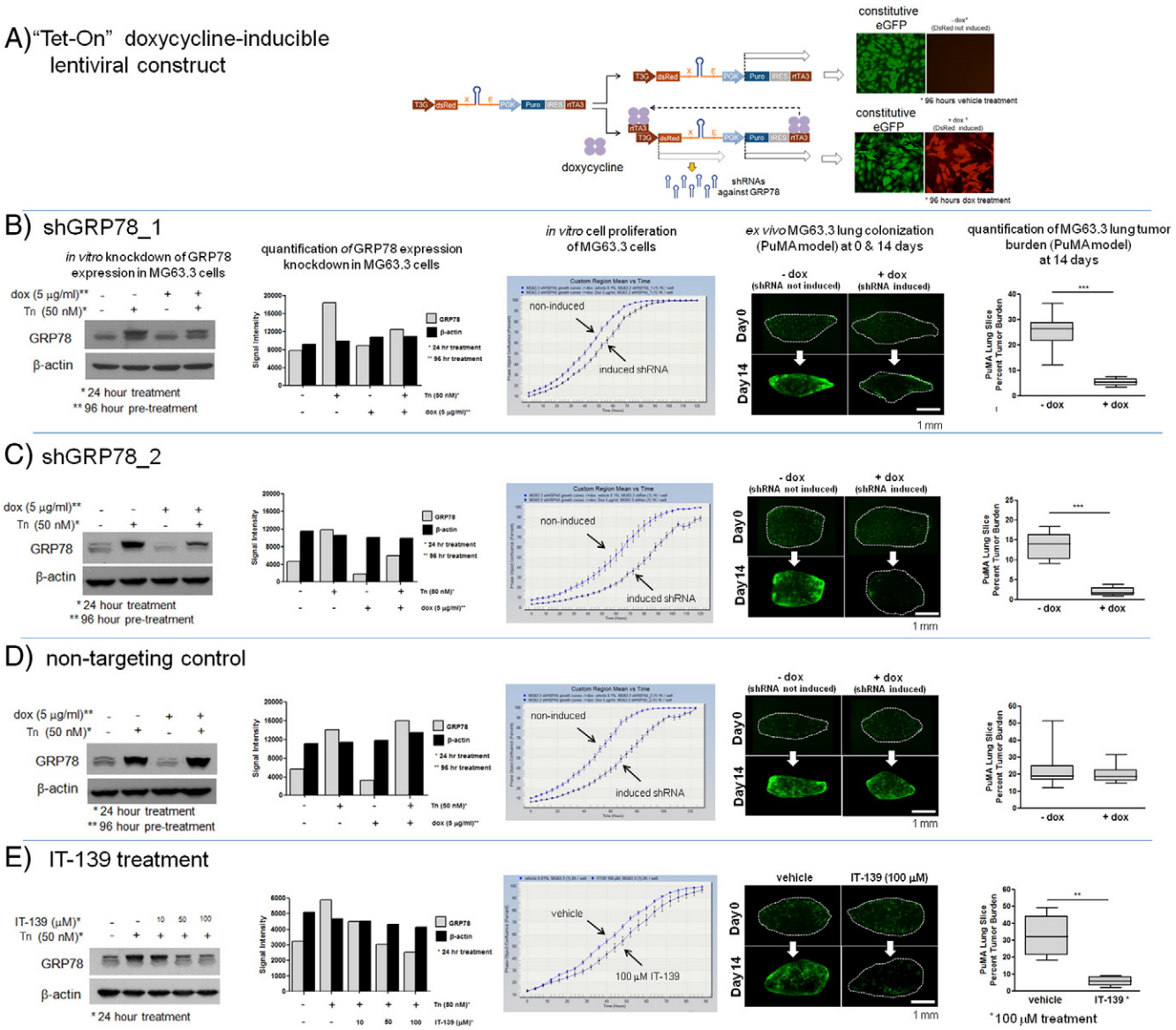


**Figure 2.** Downmodulation of GRP78 *via* genetic knockdown or pharmacologic inhibition diminishes the metastatic potential of MG63.3 cells. A schematic diagram (A) of the doxycycline-inducible shRNA construct used in these studies. (B and C) Downmodulation of GRP78 was accomplished *via* two different shRNA sequences (designated shGRP78_1 and shGRP78_2, respectively) which target the coding region of the mRNA. GRP78 protein knockdown was characterized by Western blotting; corresponding densitometry measurements are shown, where gray bars denote GRP78 protein levels and black bars denote β-actin protein levels. Induction of shRNA *via* doxycycline treatment decreased the amount of GRP78 induced by tunicamycin treatment. The effects of GRP78 downmodulation on cell proliferation were modest but inhibited metastatic outgrowth in the PuMA model. Representative fluorescence micrographs of PuMA lung slices with or without doxycycline treatment are shown for days 0 and 14. Quantification of lung tumor burden at day 14 is shown in the box and whisker plot (5%-95% percentile). Unpaired *t* test for shGRP78_1, $P < .0001$, $n = 10$; unpaired *t* test for shGRP78_2, $P < .0001$, $n = 10$. (D) A nontargeting control shRNA showed little effect on GRP78 expression, had a modest effect on *in vitro* cell proliferation, but had no significant effect on lung colonization in the PuMA model. Mann-Whitney *U* test, box and whisker plot (5%-95% percentile), $P > .05$, $n = 10$. (E) Downmodulation of GRP78 *via* IT-139 treatment. Increasing doses of IT-139 resulted in a dose-dependent knockdown of GRP78. IT-139 treatment at 100 μM did not affect *in vitro* cell proliferation but inhibited metastatic outgrowth in the PuMA model, as shown by the fluorescence micrographs. Scale bar = 1 mm. Quantification of lung tumor burden at day 14 between vehicle- and IT-139–treated PuMA lung slices is shown in box and whisker plot (5%-95% percentile). Mann-Whitney *U* test, $P < .01$, $n = 6$.

median overall survival time compared with the noninduced control group or the induced nontargeting shRNA control group (Figure 3, *B* and *C*). Representative *ex vivo* fluorescence whole-mount images which depict the disease burden in the lungs from each group are shown in Figure 3*D*. This provides evidence that targeting the ability of a metastatic to deal with the stress of a new environment, rather than the typical proliferation, is an attractive therapeutic strategy.

### *GRP78 Is Expressed in Human OS Lung Metastases*

We next asked whether GRP78 was expressed in human lung metastasis tissue. A human OS patient biopsy tissue microarray was stained for GRP78, as shown in Figure 4*A*. Of the 14 tissue cores, 8 cores had 80% to 100% of tumor cells staining positive for GRP78, 4 cores had 60% to 80% of tumor cells staining positive for GRP78, and 2 cores had 40% to 60% of tumor cells (Figure 4*B*). Human

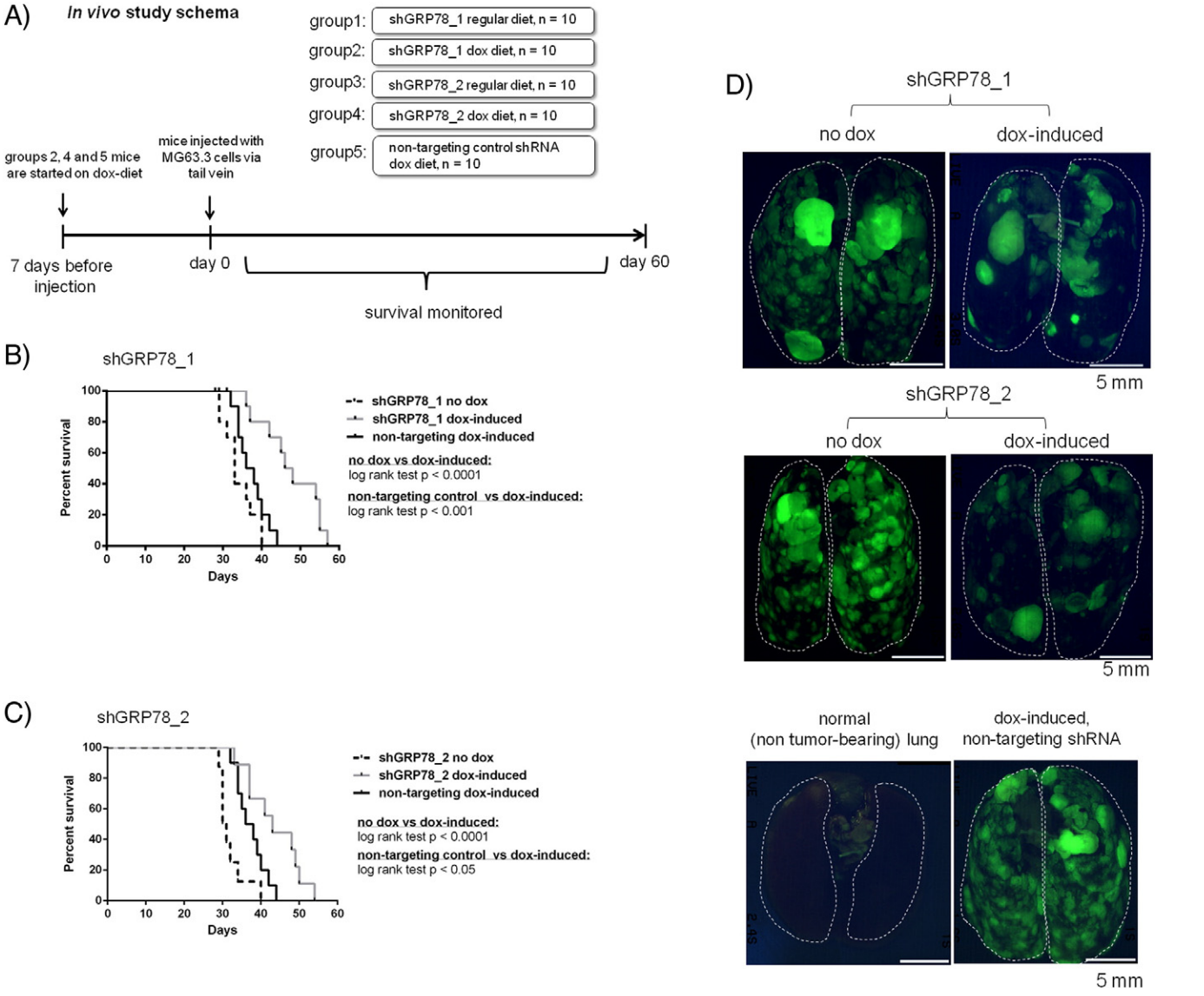


**Figure 3.** Downmodulation of GRP78 expression in metastatic MG63.3 cells *via* shRNA increases the median survival time in mice. A schematic diagram (A) of the *in vivo* experimental metastasis survival study is shown. (B) Doxycycline-induced shGRP78_1 (gray line) group exhibited a significantly longer median survival time (47 days) compared with noninduced control group (dashed line, median survival: 33 days, log-rank test $P < .0001$) and nontargeting shRNA control group (solid black line: 37 days, log-rank test $P < .001$). (C) Doxycycline-induced shGRP78_2 (gray line) group exhibited a significantly longer median survival time (43 days) compared with noninduced control group (dashed line, median survival: 31 days, log-rank test $P < .0001$) and nontargeting shRNA control group (solid black line: 37 days, log-rank test $P < .05$). (D) Representative *ex vivo* whole-mount fluorescence imaging showing the burden of disease in lungs of mice without doxycycline treatment or with doxycycline treatment. Images from the shGRP78_1, shGRP78_2, and nontargeting shRNA control are shown. A fluorescence image of a lung without tumor burden is shown for comparison.

testes strongly stained positive for GRP78 and was used as our positive control, bone tissue served a negative control, and human testes stained without primary antibodies against GRP78 served as an omission control to assess background levels of staining. It is worth noting that in nonmatched primary bone tumor cores, neoplastic cells strongly stained positive for GRP78, indicating that the stress responses required for lung metastasis are active in highly metastatic cell populations of primary tumors (data not shown).

### *GRP78 Is Required for Lung Metastasis Progression in a Murine Model of Breast Cancer Metastasis*

To assess whether upregulation of GRP78 and its link to high metastatic potential can be generalized to other types of cancers such as breast cancer, we performed similar analyses on a commonly studied, clonally related pair of murine breast cancer cell lines highly metastatic 4T1 cells and poorly metastatic 67NR cells. By confocal microscopy, 4T1 and 67NR cells had comparable levels of GRP78 when they arrived in the lung (day 0); however, at 14 days, 4T1 cells were observed to have a significantly higher staining area for GRP78 compared with 67NR cells (Figure 5*A*). By Western blotting, an enhanced upregulation of GRP78 in 4T1 cells versus 67NR cells was observed when cells were exposed to increasing concentrations of tunicamycin (Figure 5*B*). High-throughput immunofluorescence-based quantification of GRP78 expression at the single cell level (Figure 5*C*) demonstrates that highly metastatic 4T1 cells exhibited a significantly higher fold change in GRP78 expression compared with poorly metastatic

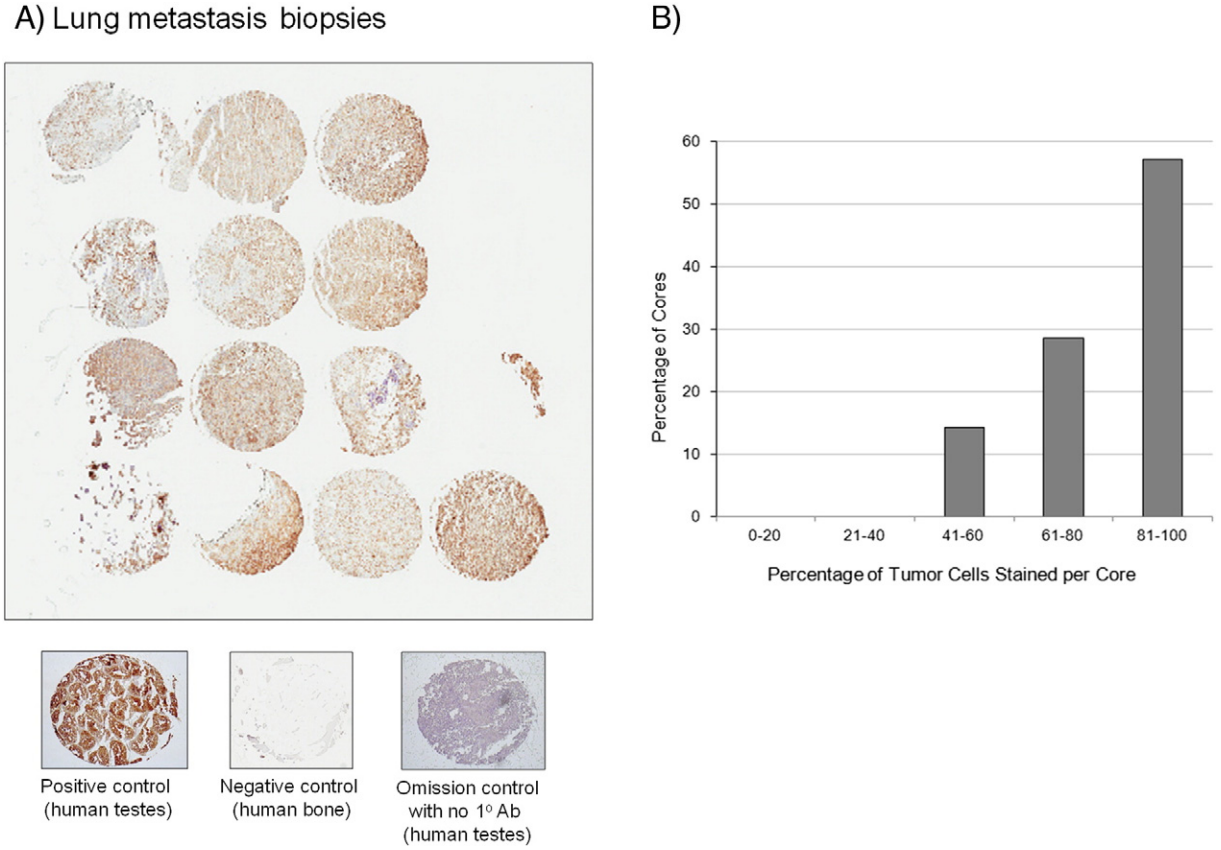


**Figure 4.** GRP78 is expressed in human OS metastatic lung tissue. (A) GRP78 is expressed in metastatic lung tissue biopsy cores from human OS patient samples. Positive staining tissue (human testes), negative control (bone), and omission control (no primary antibodies, human testes) are shown below. (B) Image quantification of the number of biopsy cores stained with OS cells staining positive for GRP78. The percentage of OS cells staining positive for GRP78 is binned on the *y*-axis. The majority of the biopsy cores had OS cells staining positive for GRP78.

67NR cells. Downmodulation of GRP78 expression in 4T1 cells was accomplished using IT-139 treatment (Figure 5*D*). Downmodulation of GRP78 did not greatly affect cell proliferation *in vitro* in the absence of any stress (Figure 5*D*); however, in the context of the lung microenvironment (PuMA model), inhibition of GRP78 significantly inhibited metastatic outgrowth (Figure 5*D*).

### *General Model of GRP78's Role in Metastatic Cancer Cell Adaptation to the Lung Microenvironment*

A diagram of how GRP78 upregulation is necessary for lung metastasis progression is shown in Figure 6. Highly metastatic cancer cells are able to adapt to microenvironmental stressors by upregulating the expression of ER-stress responsive genes such as *GRP78*, which increases the protein-folding capacity of the ER. Increased ER function permits the metastatic cancer cell to adapt and survive the adverse conditions of the lung microenvironment; this in turn is permissive for metastatic cell growth and results in a large tumor burden in the lung. Antagonizing a metastatic cancer cell's ability to adapt and survive in the lung by inhibiting GRP78 upregulation *via* genetic knockdown or drug treatment results in increased cellular stress and creates nonpermissive conditions for metastatic growth, which would result in a lower tumor burden in the lung.

## Discussion

The current report provides several lines of evidence supporting our hypothesis that ER-stress adaptation (particularly GRP78 upregulation) in highly metastatic cancer cells is causally linked to their metastatic potential. The significance of GRP78 during lung metastasis progression was first realized from our transcriptomic data where GRP78 was consistently upregulated in three different highly metastatic human OS cell lines. GRP78 is often upregulated when cells experience stressful conditions such as glucose deprivation, low ATP levels, loss of ER $Ca^{2+}$ stores, and redox imbalance [31]. We wanted to determine whether the difference in GRP78 expression between highly metastatic cancer cells and poorly metastatic cancer cells can be recapitulated *in vitro* by challenging the cells with pharmacological inducers of ER stress. Indeed, highly metastatic cancer cells consistently exhibited a robust upregulation of GRP78, whereas poorly metastatic cancer cells did not upregulate GRP78 to the same extent. Altogether, these results suggest that highly metastatic cells show a greater degree of adaptability in stressful conditions, which may explain why highly metastatic cells are more successful at colonizing the lung compared with poorly metastatic cells.

Definitive evidence for the biological relevance of GRP78 expression during metastatic progression comes from our knockdown studies where metastatic outgrowth in the lung was inhibited. Although our drug and shRNA knockdown strategies managed to partially knock down GRP78 in several highly metastatic cell lines, this partial knockdown was sufficient enough to inhibit metastatic growth in the PuMA model. These observations suggest that complete knockdown of GRP78 levels may not be necessary to have antimetastatic activity, and this information would be useful in the

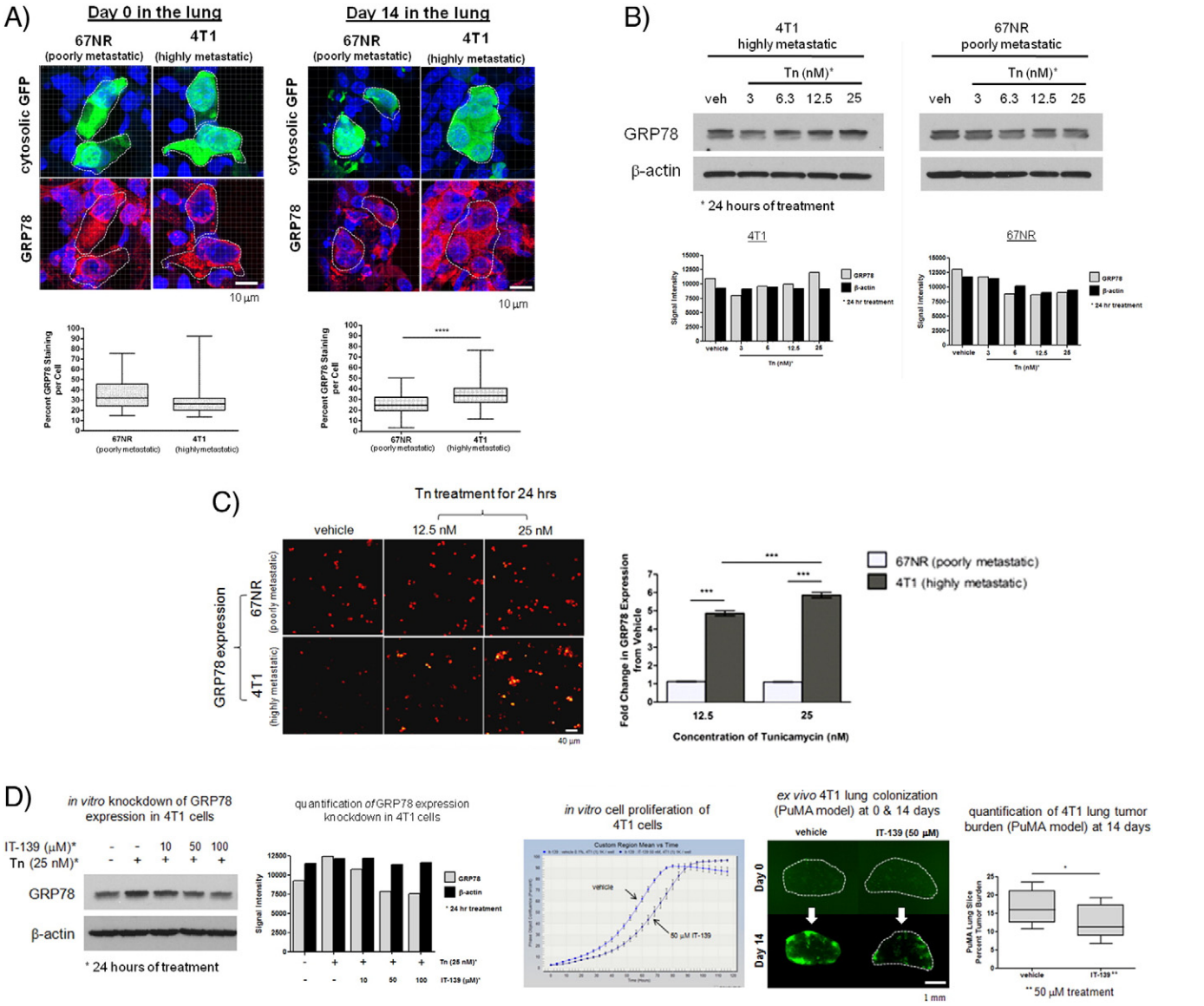


**Figure 5.** Downmodulation of GRP78 in highly metastatic murine mammary adenocarcinoma 4T1 cells *via* pharmacologic inhibition diminishes their metastatic potential in the lung. (A) Image analysis of GRP78 staining area per tumor cell in confocal images of tissue sections of paraffin-embedded, formalin-fixed PuMA lung tissue. Tissue sections from PuMA lung slices with 4T1 or 67NR were stained at day 0 and day 14 postinjection. Dashed white lines delineate where GFP-expressing murine breast cancer cells are located, and the corresponding GRP78 expression in the cancer cells is shown below. Scale bar = 10 $\mu$m. Quantification of the mean area of GRP78 staining per tumor cell for 4T1 and 67NR cells is shown for day 0 and day 14 in the PuMA model; shown in the box and whisker plot (5%-95% percentile) below the confocal images. Mann-Whitney *U* test, $P < .0001$. (B) Western blots demonstrating the *in vitro* enhanced upregulation of GRP78 in 4T1 cells versus 67NR cells upon 24-hour treatment with tunicamycin (with concentrations indicated). (C) High-throughput, image cytometry-based immunofluorescence quantification of GRP78 expression in 4T1 and 67NR cells treated with tunicamycin (12.5 nM and 25 nM) for 24 hours. Representative micrographs of each condition are shown. Scale bar = 40 $\mu$m. Quantification of the fold-change in the fluorescence due to GRP78 expression (normalized to vehicle) is shown in the adjacent bar graphs; mean and standard error are shown. Kruskal-Wallis test, $P < .0001$; Dunn's multiple comparisons test, $P < .05$. (D) Pharmacologic downmodulation of GRP78 *via* IT-139 treatment. Increasing doses of IT-139 resulted in a dose-dependent knockdown of GRP78. IT-139 treatment at 50 $\mu$M did not affect *in vitro* cell proliferation but inhibited metastatic outgrowth in the PuMA model, as shown by the fluorescence micrographs. Scale bar = 1 mm. Quantification of lung tumor burden at day 14 is shown between vehicle- and IT-139–treated PuMA lung slices; shown in the box and whisker plot (5%-95% percentile). Mann-Whitney *U* test, $P < .01$, $n = 6$.

development of novel antimetastatic therapeutics. This is evident in our *in vivo* studies where GRP78 partial knockdown *via* shRNA in highly metastatic cancer cells resulted in longer median survival times in mice.

GRP78 is a multifunctional protein that facilitates nascent protein translocation into the ER, protein folding within the ER, and binding to ER $Ca^{2+}$. More importantly, GRP78 has a critical role in ER stress response because it functions to bind and inactivate three ER stress "sensors" that initiate of ER-stress responses (IRE1, PERK, and ATF6) [31–33]. The data from our studies suggest that the lung causes upregulation of GRP78 in highly metastatic OS cells, although the exact cause(s) of GRP78 upregulation remains unclear. The requirement of GRP78 upregulation for metastatic cancer cell survival

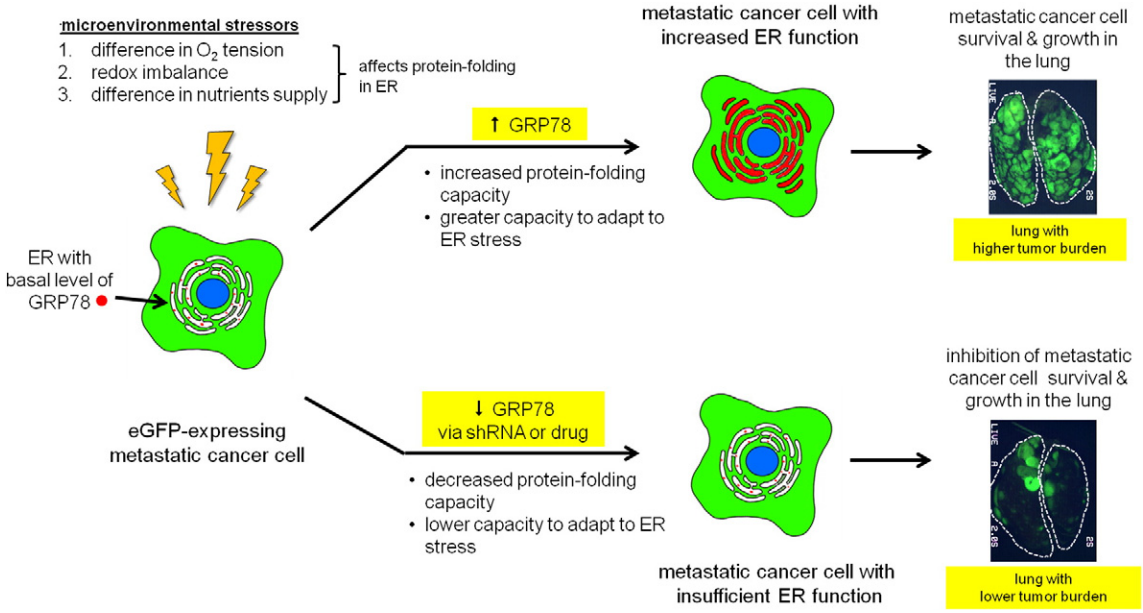


**Figure 6.** A diagram that illustrates a proposed model of how GRP78 upregulation in highly metastatic cancer cells contributes to metastatic progression in the lung. Upon arrival in the lung, highly metastatic cancer cells experience microenvironmental stressors (higher $O_2$ tension, redox imbalance, difference in nutrients supply) that can negatively protein folding and chaperone activity in the ER. Highly metastatic cancer cells adapt to these stresses by increasing ER chaperone capacity by upregulating GRP78 expression. Increased ER function allows the cancer cell to maintain cellular homeostasis which permits survival and growth in the lung. GRP78 upregulation is linked to metastatic potential because downmodulation of GRP78 expression *via* shRNA or IT-139 drug treatment results in lower metastatic outgrowth in the lung, thereby increasing median survival times in our *in vivo* experimental metastasis model.

and growth in the lung is consistently seen in human and murine cell models and in both OS and breast cancer cells. Furthermore, we demonstrated that the small molecule drug IT-139 has antimetastatic activity in the *ex vivo* PuMA model. These data support the biological relevance of the target, but further studies are needed to explore dose and regimen before this pharmacological agent can be translated into human adjuvant trials that target metastatic progression. It would be worthwhile to assess whether other GRP78-targeting chemical compounds such as HA15 [34] and medicarpin [35] have antimetastatic effects. Bioconjugates such as Mab159 [36] and BMTP78 [37] that target GRP78 have been shown to have antimetastatic effects. It is important to note that although our data may be relevant to many cancers, the result in pediatric OS addresses a critical and unmet need in the field.

To conclude, this report is the first to demonstrate a causal link between upregulated GRP78 expression and metastatic potential. We propose that GRP78 upregulation is an important adaptive response used by highly metastatic cancer cells when they disseminate to the lung and is a critical driver for lung metastatic progression. Therefore, GRP78 is an attractive target deserving of additional translational studies in the setting of inhibition of lung metastasis progression.

Supplementary data to this article can be found online at http://dx.doi.org/10.1016/j.neo.2016.09.001.

## Acknowledgements

The authors would like to thank Dr. Karen Wolcott of the Flow Cytometry Core Facility for her services. The authors would also like to thank Dr. Glenn Merlino, Dr. Allan Weissman, Dr. Kerrie Marie, Dr. Prasanna Satpute, and Cindy Clark of the NIH Library Writing Center for their critical review of the manuscript. We would like to thank Intezyne for providing IT-139 for our drug studies.

## References

[1] Langley RR and Fidler IJ (2011). The seed and soil hypothesis revisited—the role of tumor-stroma interactions in metastasis to different organs. *Int J Cancer* **128**, 2527–2535.

[2] Steeg PS (2012). Perspective: the right trials. *Nature* **485**, S58–S59.

[3] Khanna C, Fan TM, Gorlick R, Helman LJ, Kleinerman ES, Adamson PC, Houghton PJ, Tap WD, Welch DR, and Steeg PS, et al (2014). Toward a drug development path that targets metastatic progression in osteosarcoma. *Clin Cancer Res* **20**, 4200–4209.

[4] Hong SH, Ren L, Mendoza A, Eleswarapu A, and Khanna C (2012). Apoptosis resistance and PKC signaling: distinguishing features of high and low metastatic cells. *Neoplasia* **14**, 249–258.

[5] Khanna C, Wan X, Bose S, Cassaday R, Olomu O, Mendoza A, Yeung C, Gorlick R, Hewitt SM, and Helman LJ (2004). The membrane-cytoskeleton linker ezrin is necessary for osteosarcoma metastasis. *Nat Med* **10**, 182–186.

[6] Ren L, Hong SH, Chen QR, Briggs J, Cassavaugh J, Srinivasan S, Lizardo MM, Mendoza A, Xia AY, and Avadhani N, et al (2012). Dysregulation of ezrin phosphorylation prevents metastasis and alters cellular metabolism in osteosarcoma. *Cancer Res* **72**, 1001–1012.

[7] Fidler IJ (1970). Metastasis: quantitative analysis of distribution and fate of tumor embolilabeled with 125 I-5-iodo-2′-deoxyuridine. *J Natl Cancer Inst* **45**, 773–782.

[8] Wong CW, Lee A, Shientag L, Yu J, Dong Y, Kao G, Al-Mehdi AB, Bernhard EJ, and Muschel RJ (2001). Apoptosis: an early event in metastatic inefficiency. *Cancer Res* **61**, 333–338.

[9] Qiu H, Orr FW, Jensen D, Wang HH, McIntosh AR, Hasinoff BB, Nance DM, Pylypas S, Qi K, and Song C, et al (2003). Arrest of B16 melanoma cells in the mouse pulmonary microcirculation induces endothelial nitric oxide synthase-dependent nitric oxide release that is cytotoxic to the tumor cells. *Am J Pathol* **162**, 403–412.

[10] Hedley BD, Welch DR, Allan AL, Al-Katib W, Dales DW, Postenka CO, Casey G, Macdonald IC, and Chambers AF (2008). Downregulation of osteopontin contributes to metastasis suppression by breast cancer metastasis suppressor 1. *Int J Cancer* **123**, 526–534.

[11] Mendoza M and Khanna C (2009). Revisiting the seed and soil in cancer metastasis. *Int J Biochem Cell Biol* **41**, 1452–1462.

[12] Wang M and Kaufman RJ (2014). The impact of the endoplasmic reticulum protein-folding environment on cancer development. *Nat Rev Cancer* **14**, 581–597.
[13] Szegezdi E, Logue SE, Gorman AM, and Samali A (2006). Mediators of endoplasmic reticulum stress-induced apoptosis. *EMBO Rep* **7**, 880–885.
[14] Giampietri C, Petrungaro S, Conti S, Facchiano A, Filippini A, and Ziparo E (2015). Cancer microenvironment and endoplasmic reticulum stress response. *Mediators Inflamm* **2015**, 417281.
[15] Ma Y and Hendershot LM (2004). The role of the unfolded protein response in tumour development: friend or foe? *Nat Rev Cancer* **4**, 966–977.
[16] Li J and Lee AS (2006). Stress induction of GRP78/BiP and its role in cancer. *Curr Mol Med* **6**, 45–54.
[17] Roller C and Maddalo D (2013). The molecular chaperone GRP78/BiP in the development of chemoresistance: mechanism and possible treatment. *Front Pharmacol* **4**, 10.
[18] Gifford JB, Huang W, Zeleniak AE, Hindoyan A, Wu H, Donahue TR, and Hill R (2016). Expression of GRP78, master regulator of the unfolded protein response, increases chemoresistance in pancreatic ductal adenocarcinoma. *Mol Cancer Ther* **15**, 1043–1052.
[19] Zhou H, Zhang Y, Fu Y, Chan L, and Lee AS (2011). Novel mechanism of anti-apoptotic function of 78-kDa glucose-regulated protein (GRP78): endocrine resistance factor in breast cancer, through release of B-cell lymphoma 2 (BCL-2) from BCL-2-interacting killer (BIK). *J Biol Chem* **286**, 25687–25696.
[20] Aslakson CJ and Miller FR (1992). Selective events in the metastatic process defined by analysis of the sequential dissemination of subpopulations of a mouse mammary tumor. *Cancer Res* **52**, 1399–1405.
[21] Ren L, Mendoza A, Zhu J, Briggs JW, Halsey C, Hong ES, Burkett SS, Morrow J, Lizardo MM, and Osborne T, et al (2015). Characterization of the metastatic phenotype of a panel of established osteosarcoma cells. *Oncotarget* **6**, 29469–29481.
[22] Morrow JJ, Saiakhova A, Lizardo MM, Bartels CF, Bayles I, Hung S, Mendoza A, Myers JT, Allen F, and DiFeo A, et al (2015). Positively selected enhancer elements endow tumor cells with metastatic competence. *Nature* (in review).
[23] Misiewicz M, Dery MA, Foveau B, Jodoin J, Ruths D, and LeBlanc AC (2013). Identification of a novel endoplasmic reticulum stress response element regulated by XBP1. *J Biol Chem* **288**, 20378–20391.
[24] Underwood EE (1970). Quantitative stereology, vol. Addison-Wesley Pub. Co; 1970 .
[25] Fellmann C, Hoffmann T, Sridhar V, Hopfgartner B, Muhar M, Roth M, Lai DY, Barbosa IA, Kwon JS, and Guan Y, et al (2013). An optimized microRNA backbone for effective single-copy RNAi. *Cell Rep* **5**, 1704–1713.
[26] Trondl R, Heffeter P, Kowol CR, Jakupec MA, Berger W, and Keppler BK (2014). NKP-1339, the first ruthenium-based anticancer drug on the edge to clinical application. *Chem Sci* **5**, 2925–2932.
[27] Mendoza A, Hong SH, Osborne T, Khan MA, Campbell K, Briggs J, Eleswarapu A, Buquo L, Ren L, and Hewitt SM, et al (2010). Modeling metastasis biology and therapy in real time in the mouse lung. *J Clin Invest* **120**, 2979–2988.
[28] Osborne TS, Ren L, Healey JH, Shapiro LQ, Chou AJ, Gorlick RG, Hewitt SM, and Khanna C (2011). Evaluation of eIF4E expression in an osteosarcoma-specific tissue microarray. *J Pediatr Hematol Oncol* **33**, 524–528.
[29] Myhill N, Lynes EM, Nanji JA, Blagoveshchenskaya AD, Fei H, Carmine Simmen K, Cooper TJ, Thomas G, and Simmen T (2008). The subcellular distribution of calnexin is mediated by PACS-2. *Mol Biol Cell* **19**, 2777–2788.
[30] Freiden PJ, Gaut JR, and Hendershot LM (1992). Interconversion of three differentially modified and assembled forms of BiP. *EMBO J* **11**, 63–70.
[31] Lee AS (2005). The ER chaperone and signaling regulator GRP78/BiP as a monitor of endoplasmic reticulum stress. *Methods* **35**, 373–381.
[32] Zhu G and Lee AS (2015). Role of the unfolded protein response, GRP78 and GRP94 in organ homeostasis. *J Cell Physiol* **230**, 1413–1420.
[33] Lee AS (2014). Glucose-regulated proteins in cancer: molecular mechanisms and therapeutic potential. *Nat Rev Cancer* **14**, 263–276.
[34] Cerezo M, Lehraiki A, Millet A, Rouaud F, Plaisant M, Jaune E, Botton T, Ronco C, Abbe P, and Amdouni H, et al (2016). Compounds triggering ER stress exert anti-melanoma effects and overcome BRAF inhibitor resistance. *Cancer Cell* **29**, 805–819.
[35] Kureel J, John AA, Raghuvanshi A, Awasthi P, Goel A, and Singh D (2016). Identification of GRP78 as a molecular target of medicarpin in osteoblast cells by proteomics. *Mol Cell Biochem* **418**, 71–80.
[36] Liu R, Li X, Gao W, Zhou Y, Wey S, Mitra SK, Krasnoperov V, Dong D, Liu S, and Li D, et al (2013). Monoclonal antibody against cell surface GRP78 as a novel agent in suppressing PI3K/AKT signaling, tumor growth, and metastasis. *Clin Cancer Res* **19**, 6802–6811.
[37] Miao YR, Eckhardt BL, Cao Y, Pasqualini R, Argani P, Arap W, Ramsay RG, and Anderson RL (2013). Inhibition of established micrometastases by targeted drug delivery via cell surface-associated GRP78. *Clin Cancer Res* **19**, 2107–2116.